creative commons
COMMONS DEED

저작자표시-비영리-변경금지 2.0 대한민국

이용자는 아래의 조건을 따르는 경우에 한하여 자유롭게

- 이 저작물을 복제, 배포, 전송, 전시, 공연 및 방송할 수 있습니다.

다음과 같은 조건을 따라야 합니다:

저작자표시. 귀하는 원저작자를 표시하여야 합니다.

비영리. 귀하는 이 저작물을 영리 목적으로 이용할 수 없습니다.

변경금지. 귀하는 이 저작물을 개작, 변형 또는 가공할 수 없습니다.

- 귀하는, 이 저작물의 재이용이나 배포의 경우, 이 저작물에 적용된 이용허락조건을 명확하게 나타내어야 합니다.
- 저작권자로부터 별도의 허가를 받으면 이러한 조건들은 적용되지 않습니다.

저작권법에 따른 이용자의 권리는 위의 내용에 의하여 영향을 받지 않습니다.

이것은 이용허락규약(Legal Code)을 이해하기 쉽게 요약한 것입니다.

Disclaimer

dCollection

공학석사 학위논문

Photosensitivity of InZnO thin-film transistors using a solution process

용액 공정을 이용한 InZnO 박막트랜지스터의 광전 감도에 관한 연구

2016년 8월

서울대학교 대학원

융합과학부 나노융합전공

최 종 원

Photosensitivity of InZnO thin-film transistors using a solution process

지도 교수 김 연 상

이 논문을 공학석사 학위논문으로 제출함
2016 년 4 월

서울대학교 대학원
융합과학부 나노융합전공
최 종 원

최종원의 석사 학위논문을 인준함
2016 년 7 월

위 원 장 박 원 철 (인)

부위원장 김 연 상 (인)

위 원 이 강 원 (인)

Abstract

Photosensitivity of InZnO thin-film transistors using a solution process

Jongwon Choi
Program in Nanoscience and Technology
The Graduate School of
Seoul National University

Amorphous silicon (a-Si) and low temperature polysilicon (LTPS) TFTs are extensively used in the flat-panel display industry, but they have a number of disadvantages. Alternatively, oxide semiconductors have been researched for more than a decade as a promising active material for TFTs. Recent electronic devices have been widely utilized with interactive technology to allow interaction with the user. One typical example is interactive display technology combined with a TFT and a sensor. In view of this, oxide semiconductor devices play a

role in both switches and photo-sensors in interactive displays. However, most studies of oxide photo-transistors have concentrated on oxide semiconductors made by a vacuum process. During the fabrication of oxide semiconductor devices, the sol-gel solution process used to form an oxide semiconductor has various merits, including its simplicity and low cost as well as its good composition controllability.

Here, we present the photosensitivity characteristics of an oxide photo thin-film transistor (TFT) created using the InZnO (IZO) sol-gel process. Upon exposure to light, photocurrent (I_{photo}) in the negative gate bias regime is significantly increased with a negligible threshold voltage shift. The photosensitivity is modulated by geometrical factors and by the IZO material composition. We observed a significant effect of the channel thickness and IZO composition on the photosensitivity which was attributed to the screening effect of optically ionized oxygen vacancies (V_o^{++}). Particularly, the optimized bi-layered oxide photo-TFT presents a good I_{photo}/I_{dark} photosensitivity value of $3x10^4$ and a subthreshold slope of 0.96V/decade. In addition, the persistent photoconductivity of the oxide photo-TFT was removed by applying

positive gate voltage, resulting in good high-speed operation. These results taken together demonstrate that the IZO photo-TFT produced by the sol-gel process can be successfully when applied to interactive displays.

Keywords: thin-film transistor, oxide semiconductor, photosensitivity, photo-sensor, solution process, oxygen vacancy

Student Number: 2014-24886

Contents

List of Figures

Figure 7. Transfer characteristics of the photo-transistor at different channel lengths (L = 10, 20, 30, 40 and 50 μm).

Figure 8. (a) Changes in the EQE and responsivity of the device according to the thickness of the $I_{0.7}Z_{0.3}O$ film. (b) Calculated EQE and responsivity values at different channel lengths.

Figure 9. Transfer characteristics of IZO TFTs with the In:Zn composition of 7:3, 5:5 and 3:7 in the dark and under illumination.

Figure 10. I_{DS}-V_{GS} sweeps of IZO TFT (hysteresis sweeps) with three types of IZO composition (In:Zn=7:3, 5:5, 3:7). The directions of the forward and reverse sweeps are indicated. (V_{DS} = 10 V)

Figure 11. Measured Tauc plots of IZO layers as a function of the In:Zn composition.

Figure 12. Transfer characteristics of the photo-transistors with the In:Zn compositions of 7:3(mono) and 5:5(mono) and the bi-layer composition ($I_{0.5}Z_{0.5}O$ + $I_{0.7}Z_{0.3}O$).

Figure 13. Dynamic photoresponse characteristics of the IZO TFT when the devices are subjected to light and gate bias pulses, where a positive top bias of 10 V is applied as a reset operation after applying a pulse base bias of -10 V.

List of Tables

Chapter 1. Introduction

1.1 Oxide thin-film transistors & photo-transistors

Recently, amorphous/nano-crystalline Zn-based oxide semiconductor thin-film transistors (TFTs) have been attracting tremendous amounts of attention. The oxide semiconductor TFT has numerous outstanding attributes, including high mobility, a wide band-gap, low-temperature processability and a low leakage current level.[1-4] In particular, the high mobility of an oxide semiconductor makes it applicable to high-speed electronic devices.[5,6] In addition to being used as a switching device, the InZnO semiconductor material, which possesses a wide band-gap (~3 eV) with a certain number of sub-gap states, can be used as an active material in photo-TFTs, especially for visible light photo-sensors and image sensors.[7,8] Depending on the process condition, the optical band-gap and sub-gap oxygen vacancy states are tunable, allowing the realization of a highly sensitive photo- sensor.[9] Considering the fact that the oxide component can be used for the switch and for the sensor, it can serve as the core device element in interactive displays which are capable of interacting with users.

1.2 Solution-processed IZO photo-transistors

With increasing interest in oxide semiconductor materials owing to their high mobility levels and attractive optical properties, fabrication methods with these materials have been studied in various ways.[10] In early studies, oxide semiconductor thin films were mostly prepared by expensive vacuum processes such as pulsed laser deposition and sputtering owing to the good uniformity of the film.[11] However, the vacuum deposition method has several disadvantages, such as its high fabrication cost and limited deposition area. On the other hand, the solution method presents the advantages of simplicity and a low manufacturing cost. Moreover, the excellent throughput and homogeneity as well the as easy compositional controllability make the solution process a promising thin-film fabrication technology.[12] However, thus far most studies of oxide photo-transistors have relied on vacuum processes.[13,14] Herein, we employ a sol-gel process based on zinc nitrate and indium nitrate as a solution process for the forming of IZO as a semiconductor material.

In this study, we examine the photo-response characteristics of oxide photo-TFTs with IZO prepared by a sol-gel process. The photo-current ratio (I_{photo}/I_{dark}) was enhanced by adjusting the geometrical factors

and the IZO material composition. We found that the effect of the IZO semiconductor thickness (T_{IZO}) and the cation amount ratio (In:Zn) on the photosensitivity are significant, as explained by the screening effect of the light-induced doubly positively charged oxygen vacancies (V_o^{++}). We also noted that the metal cation contents in IZO were critical for determining the high photosensitivity and interfacial quality. Better photosensitivity was observed with $In_{0.5}Zn_{0.5}$, while good transistor performance observed with $In_{0.7}Zn_{0.3}$. Thus, we developed a high-performance photo-sensor TFT using the In-Zn cation modulated by a double-layered channel. We also resolved the persistent photoconductivity of the IZO TFT by applying a positive gate reset voltage, leading to high-speed photo-sensor operation.

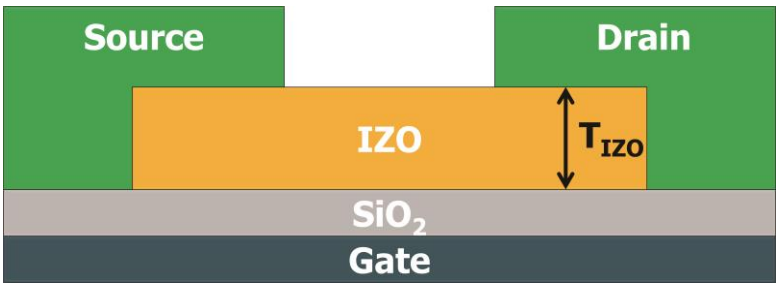

Figure 1. Structure of IZO thin-film transistors (TFTs). Schematic of the proposed TFTs consisting of bottom gate (Si) / dielectric layer (SiO_2 200 nm) / semiconducting layer (IZO) / Top electrode (Al 100 nm).

Chapter 2. Experimental process

2.1 Fabrications of IZO TFTs

The solution process for IZO TFTs is schematically presented in Figure 2. During the sol-gel IZO coating process, the precursor solution for the 0.2 M $I_{0.7}Z_{0.3}O$ thin film was synthesized by dissolving 0.84g of indium nitrate hydrate ($In(NO_3)_3 \times H_2O$, Aldrich, 99.999%) and 0.36g of zinc nitrate dihydrate ($Zn(NO_3)_2 \times H_2O$, Aldrich, 99.999%) in 10ml of 2- methoxyethanol.[15] In the same way, $I_{0.5}Z_{0.5}O$ and $I_{0.3}Z_{0.7}O$ were dissolved in 2-methoxyethanol while controlling the relative molar composition. These stock solutions were stirred for 12 hours at room temperature in order to obtain a homogeneous solution, after which the solution was filtered through a PTFE filter (0.45 μm pore size) before the spin-coating process. The SiO_2 (200 nm)/ silicon (Si) substrates were used after cleaning by sonication with deionized water, acetone and isopropyl alcohol. The IZO precursor solution was spin-coated at 3000 rpm for 30 s onto the substrates. After the IZO film coating, the sample was annealed at 300℃ for 60 min on a hot plate in an ambient atmospheric environment. A conventional photolithography process was used to

pattern the IZO active layer and the top electrode. The 100 nm Al source and drain electrodes were finally deposited using a thermal evaporator and a lift-off method (Figure 1).

2.2 Characterizations of IZO TFTs

The electrical characteristics of the IZO thin-film transistors were measured using a semiconductor parameter analyzer (Agilent 4155B) and a probe station. Light with a wavelength of 400~550 nm was extracted from a xenon lamp by a monochromatic light source system. X-ray photoelectron spectroscopy (XPS) (Sigma Probe, ThermoVG) was used to characterize the electronic state of the IZO films. The thickness of the films was characterized by an ellipsometer (V-VASE, Wollam). Dynamic photoresponse measurement was performed with Agilent 81104A pulse generator.

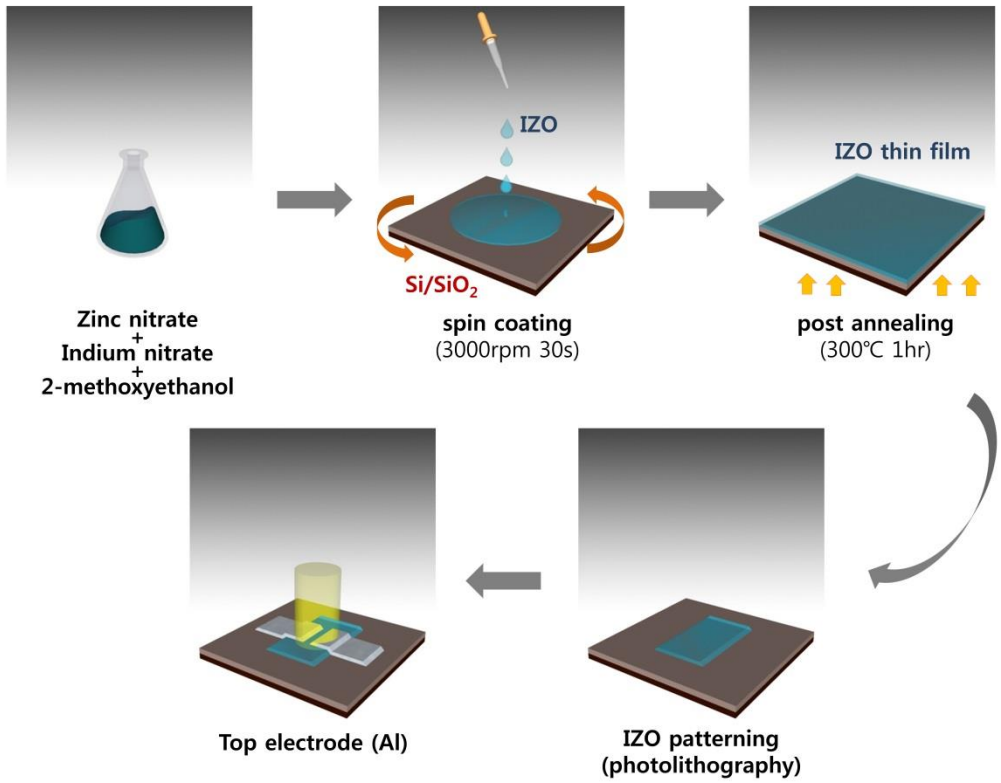

Figure 2. Schematic diagram of the solution process for IZO TFTs

Chapter 3. Results and discussion

3.1 Material property of IZO thin films

In order to confirm the material composition of the solution-processed IZO thin films, we performed X-ray photoelectron spectroscopy (XPS) study as seen in Figure 3. As shown in Figure 3, the measured XPS data shape of the In 3*d* and Zn 2*p* core levels for the IZO films are in good agreement with previous experimental data.[16,17] The In $3d_{5/2}$ peak at 444.1 eV and the Zn $2p_{3/2}$ peak at 1021.1 eV correspond to the In-O and the Zn-O bonds, respectively. Considering of peak area of In 3d and Zn 2p as well as sensitivity factor, we found that the prepared film (Figure 3) was $In_{0.7}Zn_{0.3}$. The O 1*s* core level peak was fitted to two Gaussian distributions. (Figure 3). A peak corresponding to a lower binding energy can be assigned to O^{2-} ions surrounded by In and Zn atoms, and the a peak corresponding to higher binding energy is associated with O^{2-} ions in oxygen deficient regions in the IZO compound.

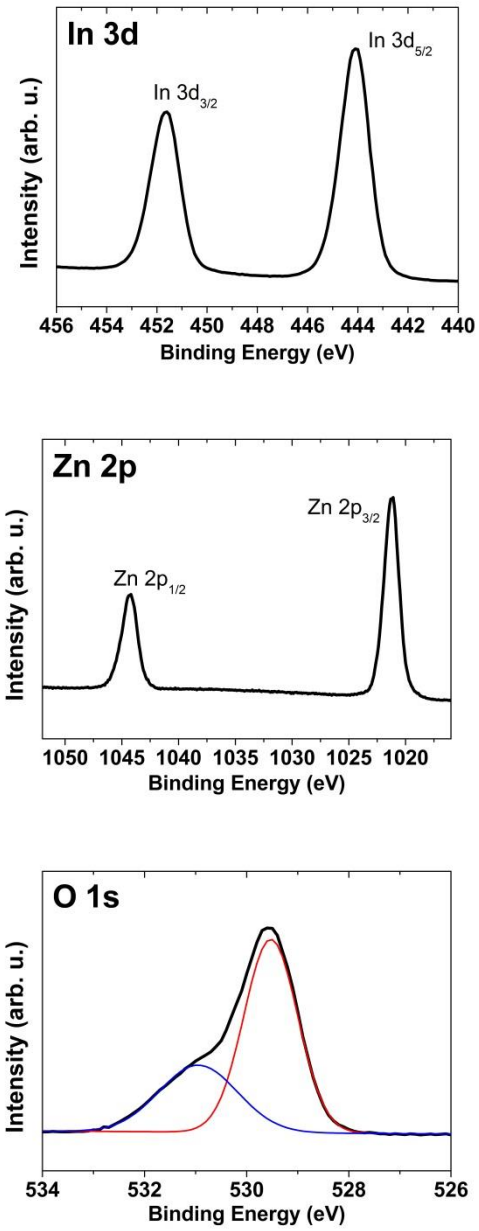

Figure 3. Schematic diagram Representative XPS spectra of In 3d, Zn 2p, and O 1s of the $I_{0.7}Z_{0.3}O$ thin film.

3.2 Photoconductivity behavior of IZO TFTs

In order to examine the photoconductivity behavior of the IZO TFT under various-wavelength (λ) light illumination, we measured I_{DS}-V_{GS} transfer curves of IZO TFT upon exposure to 400~550nm-wavelength light as seen in Figure 4. The IZO TFT shows noticeable photocurrent for the light illumination with λ of 400–475nm, while it presents negligible photocurrent for the light with λ of greater than 525 nm. In our experimental results, the IZO has a wide bandgap of 3.05eV and a certain number of sub-gap states (attributed to oxygen vacancies). Thus it indicates that the absorption in the IZO layer under the light exposure with less photon energy than 2.9eV is largely responsible for sub-gap states. A gradual increase in the photocurrent under 425-475nm (2.9-2.6eV) resulted from optically induced doubly positively charged oxygen vacancy (V_o^{++}) in the IZO layer, which weakens the influence of the negative gate bias and enhances the back channel conduction. This effect is significant for the relatively thick IZO device. Thus the thickness of IZO active semiconductor is major parameter to determine the photoconductivity.[18]

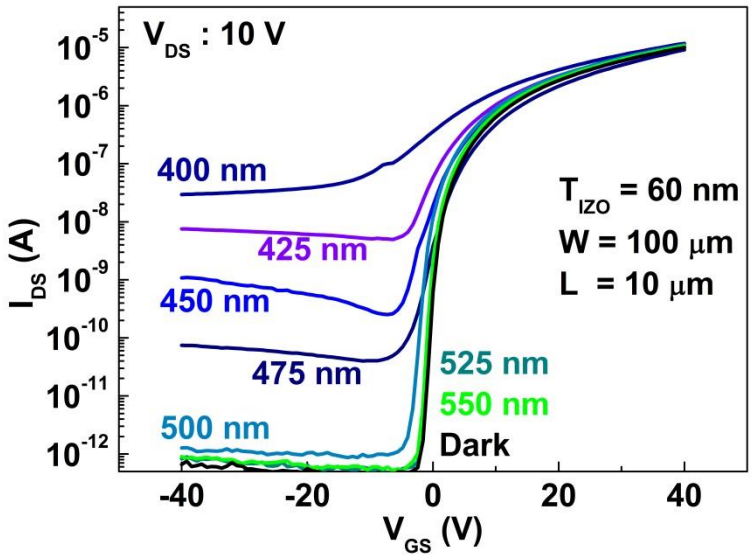

Figure 4. Transfer characteristics of $I_{0.7}Z_{0.3}O$ TFTs under exposure to 400, 425, 450, 475, 500, 525 and 550 nm light with a power of ~100 μWcm^{-2}.

3.3 Thickness dependence of IZO photo-TFTs

In order to verify the active thickness effect on the photosensitivity of the IZO TFT, the transfer curves of IZO transistors with various active thicknesses were measured under dark and illumination conditions (λ : 425 nm & optical power : 100 μWcm^{-2}.) (Figure 5). The thickness of each film was controlled by the number of spin-coating trials, where one, two, and three coatings were used correspondingly to create 30, 60, and 90 nm IZO layers, which was clarified by spectroscopic ellipsometer. With increasing the IZO active thickness, the I_{DS}-V_{GS} transfer curve of the IZO device under dark state slightly shifts toward a negative gate bias direction. The 90nm-thick IZO device shows a slight shift in threshold voltage and subthreshold slope. Here, this is not a significant change in the dark state. However, under the light illumination, there is a considerable increase in the current level at negative gate voltage depending on the IZO active thickness. As the IZO thickness was increased from 30 to 60 nm, the photocurrent ratio (I_{photo}/I_{dark}) in negative gate bias regime increased up to 10^2 to 10^5. Moreover the photocurrent of 90nm-thick IZO TFT was approximately five orders of magnitude higher than that before illumination. In order to understand these results, it is necessary

to explain the concept of a back-channel model. When the light is exposed to the IZO TFT, the neural V_o is ionized to V_o^{++} (Figure 6). As we apply negative gate voltage, V_o^{++} is primarily located in front channel. Then it screens negative gate voltage. Especially for relatively thick IZO TFT, the back channel is not totally depleted. Then, the back channel plays a major transport region under the light illumination. Thus, thick active IZO TFT shows high photoconductivity. The quantitative data regarding other photo current performance such as external quantum efficiency (EQE) and responsivity (R) will be discussed later, along with geometrical effect on photoconductivity.

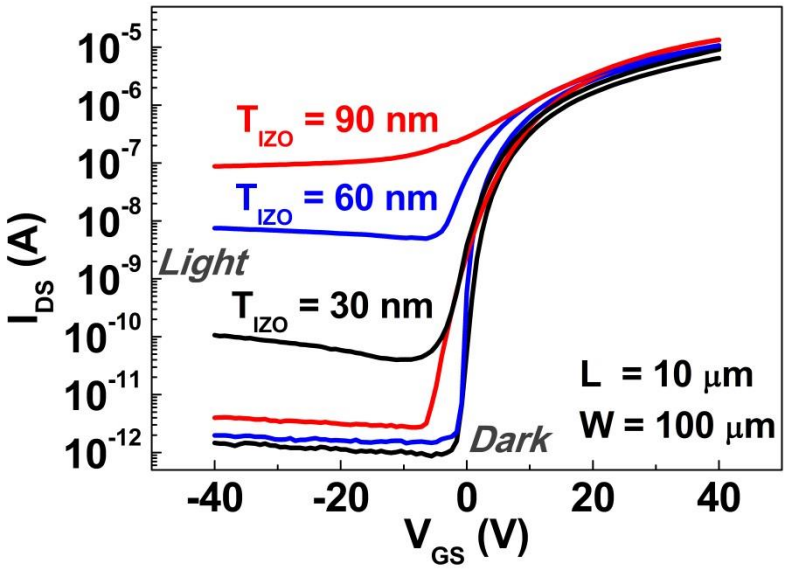

Figure 5. Transfer characteristics of $I_{0.7}Z_{0.3}O$ TFTs with T_{IZO} = 30, 60 and 90 nm in the dark and under illumination (L = 10 μm and W = 100 μm).

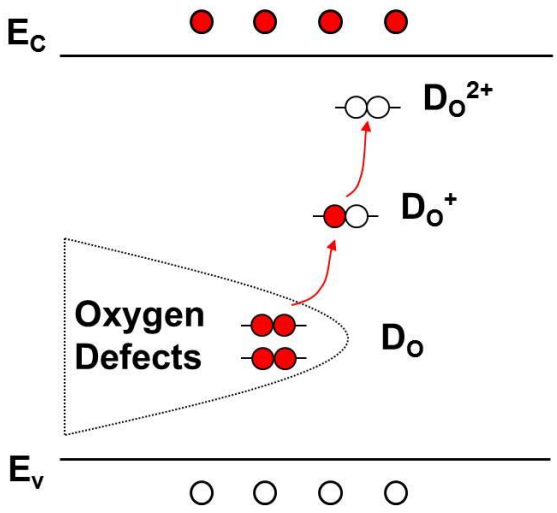

(a)

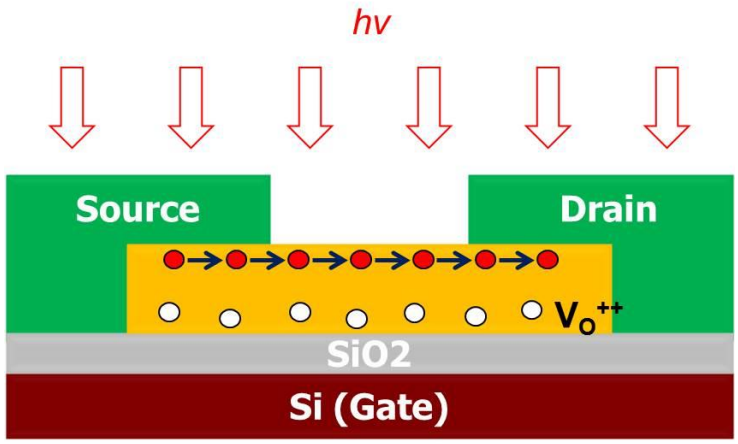

(b)

Figure 6. (a) Schematic band diagram to describe ionization of oxygen vacancy in the IZO layer. (b) Schematic illustration of the carrier profile along the channel IZO after light illumination ($V_{GS} < 0$)

3.4 Channel length dependence of IZO photo-TFTs

In order to achieve high photo conductivity gain of IZO photo-transistor, we examined the influence of a representative geometrical factor, channel length (10, 20, 30, 40 and 50μm) on photo-current characteristics of TFT device in the dark and under light illumination.[19] (Figure 7) As the channel length was decreased, as expected, the photocurrent increased. In a short-channel IZO transistor, the photo current was increased by about four orders of magnitude higher than dark current level. On the other hand, for a long channel IZO device, the photo conductivity is lower than short channel devices. So it can be speculated that a certain part of conduction region is located along with carrier transport channel for a short channel device. It suggests that the un-depleted back channel in source side is formed, thereby forming conducting channel. Optically induced V_o^{++}s can effectively significantly lowers source-to-channel barrier height in short channel length and prevent from forming a fully depleted region. As a result, a short channel device can achieve high photoconductivity gain, so the scaling of device technology can play important role in achieving high photoconductivity gain of photo sensor devices.

The EQE and responsivity in photo-sensor devices are very

important performance parameters.[10,20]

(1)

$$\mathrm{EQE} = \frac{J_{ph} / \mathrm{q}}{P / h\nu}$$

(2)

$$\text{responsivity} = \frac{J_{total} - J_{dark}}{P} = \frac{J_{ph}}{P}$$

In Equations (1) and (2), J_{total} is the total current density, J_{dark} is the dark current density, P is the incident laser power, and J_{ph} is the photo current density. The 30nm-thick IZO TFT show low EQE and responsivity as seen in Figure 8, while with increasing the IZO thickness, EQE and responsivity are increased on a logarithmic scale. Figure 8 shows the influence of channel length on EQE and responsivity. Consistent with the photocurrent as a function of channel length in Figure 8, both EQE and responsivity parameters decrease with increasing channel length, indicating that short channel length device shows high photoconductivity gain.

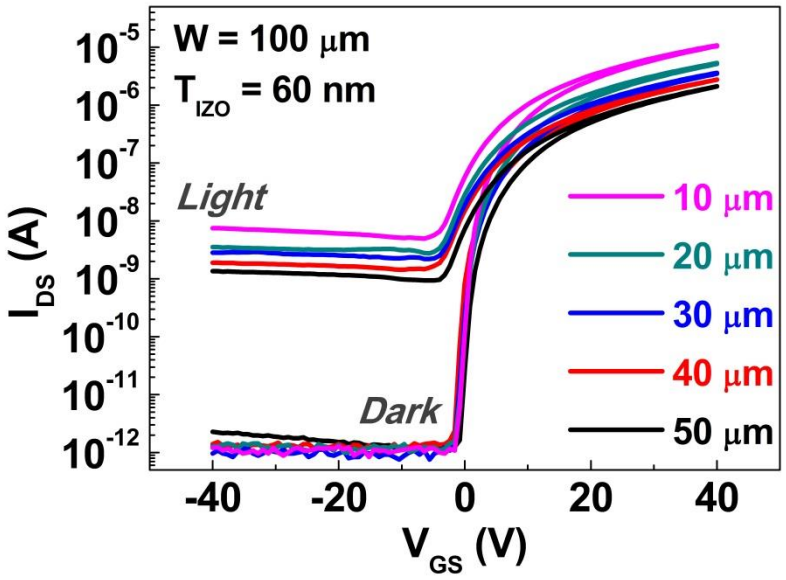

Figure 7. Transfer characteristics of the photo-transistor at different channel lengths (L = 10, 20, 30, 40 and 50 μm).

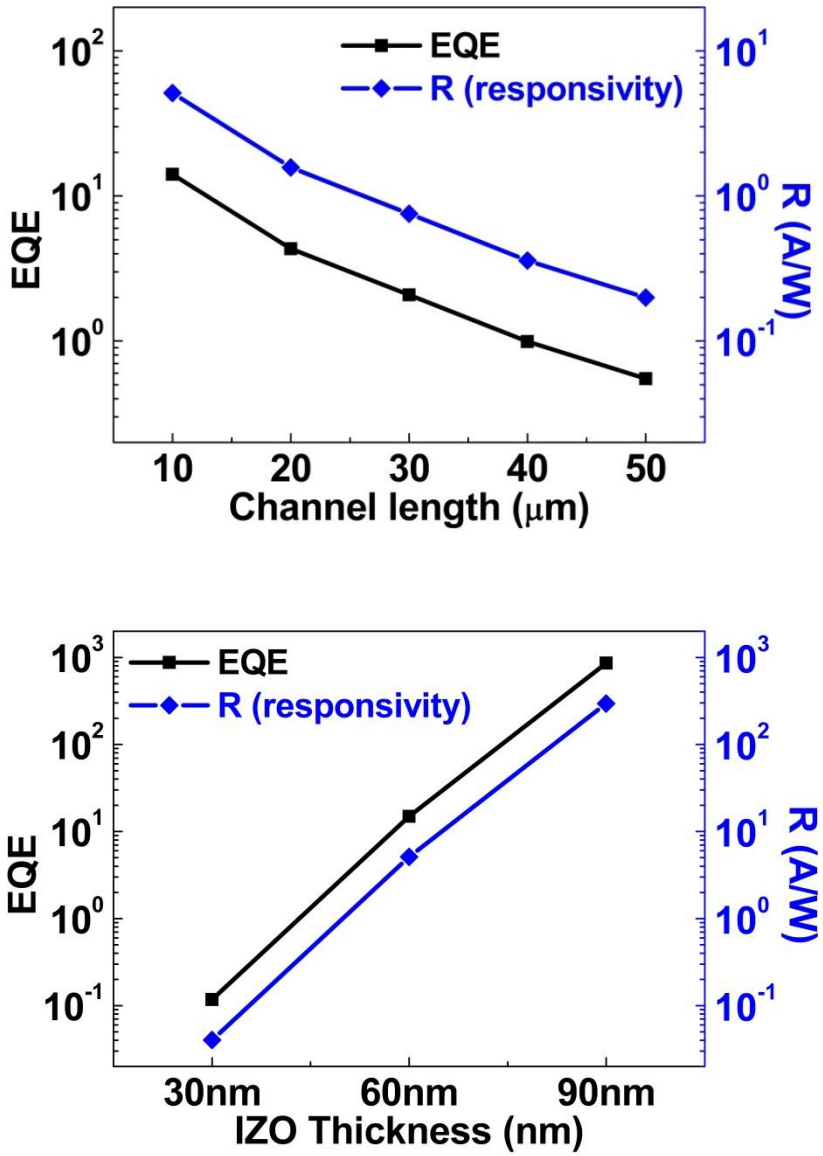

Figure 8. (a) Changes in the EQE and responsivity of the device according to the thickness of the $I_{0.7}Z_{0.3}O$ film. (b) Calculated EQE and responsivity values at different channel lengths.

3.5 In:Zn composition effect of IZO photo-TFTs

In order to study the effect of the IZO cation ratio on both electrical and photo-response characteristics of IZO TFTs, we performed the I_{DS}-V_{GS} measurements of IZO TFTs with various IZO material compositions. Figure 9 shows I_{DS}-V_{GS} transfer characteristics of IZO TFTs with three types of IZO composition (In:Zn=7:3, 5:5, 3:7) under the dark and illumination states. When increasing the zinc content with respect to indium, the on/off current ratio decreased from 10^7 to 10^5 in the dark state, the turn-on voltage (V_{on}) shifted to negative gate voltage condition and the subthreshold swing increased. However, interestingly the photocurrent properties of the devices with different compositions indicated a positive sign for a high photoconductivity gain. The $I_{0.5}Z_{0.5}O$ and $I_{0.3}Z_{0.7}O$ TFTs with an increased zinc element ratio generated more photocurrent than $I_{0.7}Z_{0.3}O$ TFT, mainly due to the ionization oxygen defects in the IZO layer. To confirm this, we measured Tauc plot of the IZO layer with different compositions, as shown in Figure 11. The $I_{0.5}Z_{0.5}O$ and $I_{0.3}Z_{0.7}O$ layers had relatively high oxygen defect states in sub-gap region (< 3 eV). However, the Zn-rich IZO TFTs showed poor transfer characteristic curves and large hysteresis voltages (Figure 10), in contrast to a stable device. Based

on these characteristics, we prepared a bi-layer channel to improve electric performance and photoconductivity at the same time. The bi-layer channel was applied with each different combination of In and Zn. To improve transistor performance, the $I_{0.7}Z_{0.3}O$ layer also served as a capping layer to achieve excellent current drivability and threshold voltage controllability. To realize high photoconductivity gain, $I_{0.5}Z_{0.5}O$ layer served as photo activation layer in the front channel area. In terms of the transfer curve in the dark, the bi-layer TFT exhibited properties similar to those of the $I_{0.7}Z_{0.3}O$ TFT. The photocurrent under illumination reached a higher level than a single layer TFT, as shown in Figure 12. Table I. summarizes the IZO material information and the electric characteristics of the IZO TFTs. The dark-state electrical performance of bi-layer IZO TFTs was found to be similar to those of $I_{0.7}Z_{0.3}O$ TFTs in the dark. Moreover, the photocurrent gain (I_{ph}/I_{dark}) of the bi-layer IZO photo-transistor surpassed than that of the $I_{0.7}Z_{0.3}O$ photo-transistor (60 nm) in the illumination condition.

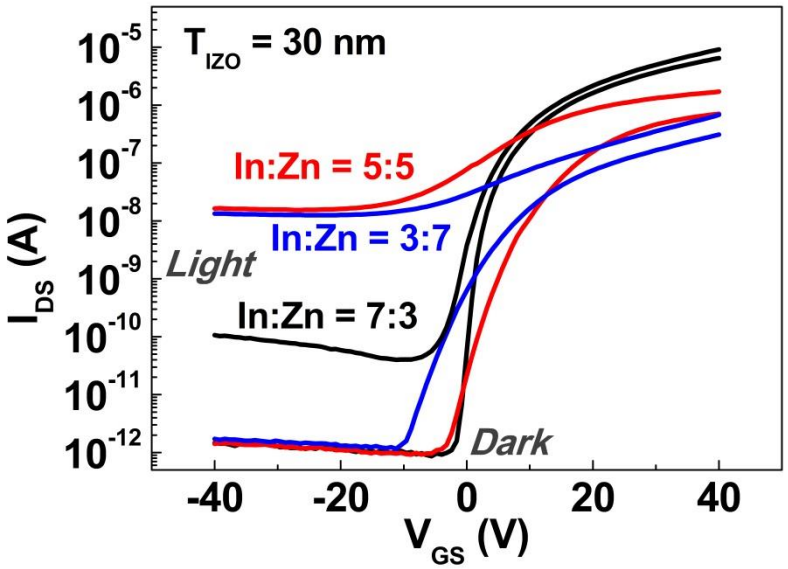

Figure 9. Transfer characteristics of IZO TFTs with the In:Zn composition of 7:3, 5:5 and 3:7 in the dark and under illumination.

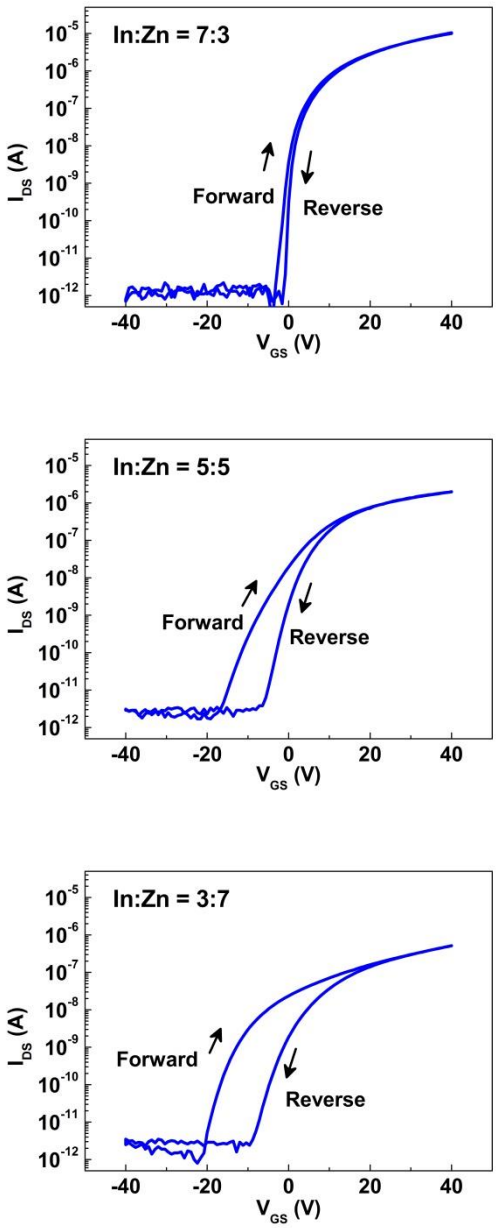

Figure 10. I_{DS}-V_{GS} sweeps of IZO TFT (hysteresis sweeps) with three types of IZO composition (In:Zn=7:3, 5:5, 3:7). The directions of the forward and reverse sweeps are indicated. (V_{DS} = 10 V)

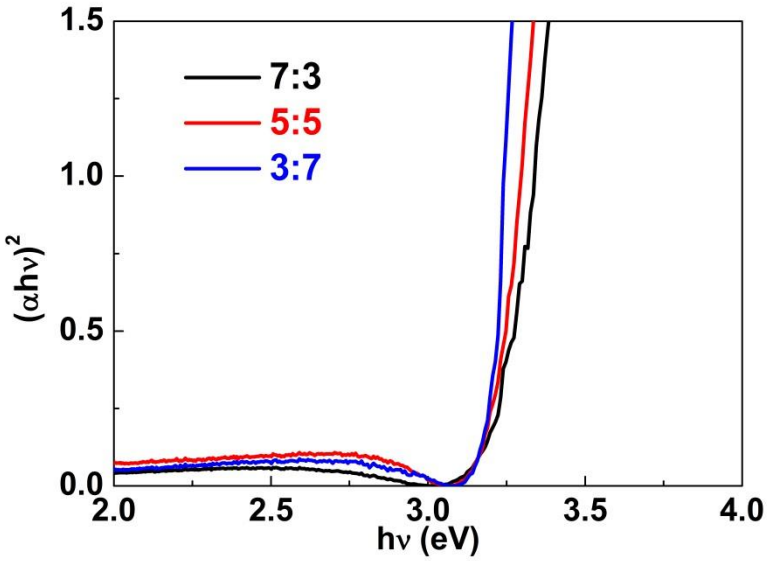

Figure 11. Measured Tauc plots of IZO layers as a function of the In:Zn composition.

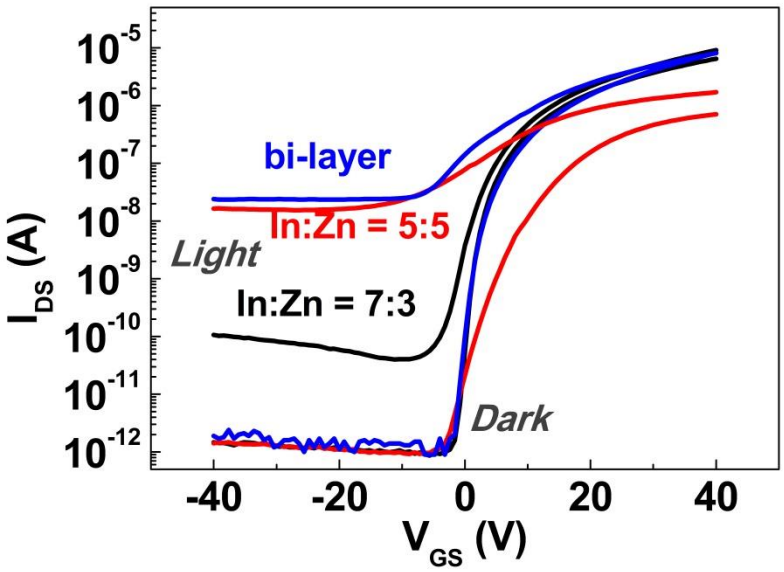

Figure 12. Transfer characteristics of the photo-transistors with the In:Zn compositions of 7:3(mono) and 5:5(mono) and the bi-layer composition ($I_{0.5}Z_{0.5}O + I_{0.7}Z_{0.3}O$).

TABLE I. Parameters extracted for IZO TFTs

In:Zn ratio	T_{IZO} (nm)	μ_{sat} ($cm^2/eV/s$)	S/S (V/dec)	V_{on} (V)	N_t ($10^{11}/cm^2/eV$)	I_{ph}/I_{dark} ratio
$I_{0.7}Z_{0.3}O$	30	1.92	0.60	-0.8	21.7	$4x10^1$
$I_{0.5}Z_{0.5}O$	30	0.58	2.41	-2.4	87.7	$2x10^4$
$I_{0.3}Z_{0.7}O$	30	0.08	4.89	-9.6	177.1	$1x10^4$
$I_{0.5}Z_{0.5}O + I_{0.7}Z_{0.3}O$	30 + 15	2.30	0.96	-0.8	34.7	$3x10^4$
$I_{0.7}Z_{0.3}O$	60	1.86	0.91	0.0	32.9	$5x10^3$

3.6 Dynamic photoresponse characteristics of solution-processed IZO photo-TFTs

Figure 13 shows the dynamic photoresponse of a solution-processed IZO TFT in a pulse illumination system. For application to actual photo-sensor arrays, the changes in the photocurrent level at a read voltage should be measured. In the dark state, the current level maintained a low current level. Upon exposure to the light illumination, photocurrent level is immediately increased. Subsequently, when the illumination was turned off, very slow recovery of the photocurrent signal was observed. This is known as persistent photoconductivity (PPC) phenomenon, which the unique characteristics of the oxide semiconductors.[21] Positively charged oxygen vacancies (V_o^{++}) are located at the front channel, and electrons are pushed to the back channel area by the electric field when in the negative gate bias condition. Thus, even after the light disappears, the recombination between the oxygen vacancies and the free electrons does not occur. A reset of the gate pulse at a positive bias can resolve the PPC problem. The change in the gate bias condition from negative bias to positive bias induced compulsory recombination with ionized oxygen vacancies and free electrons, with the photocurrent eventually

eliminated. This dynamic photoresponse measurement was performed with an Agilent 81104A pulse generator.

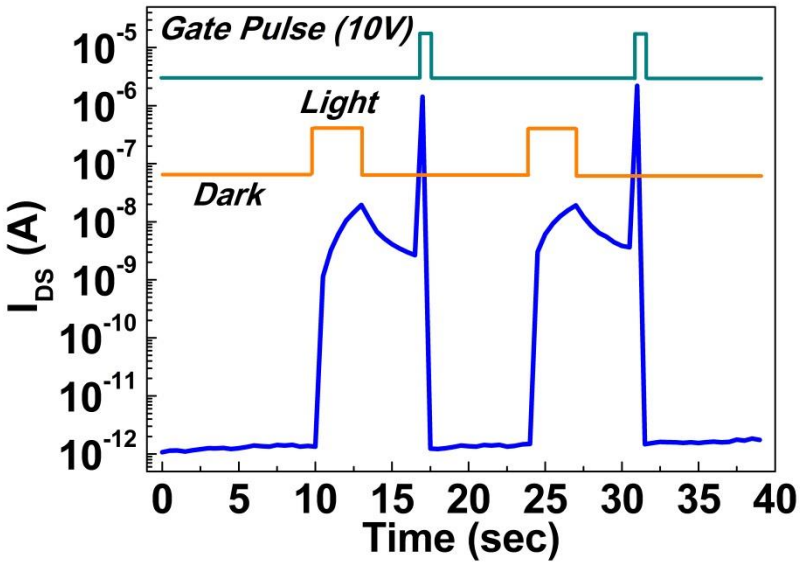

Figure 13. Dynamic photoresponse characteristics of the IZO TFT when the devices are subjected to light and gate bias pulses, where a positive top bias of 10 V is applied as a reset operation after applying a pulse base bias of -10 V.

Chapter 4. Conclusion

In summary, we investigated the photo-response characteristics of an oxide photo-TFT with IZO semiconductor layer prepared by sol-gel process based on zinc nitrate and indium nitrate. When the device is exposed to light, the photocurrent was significantly increased by several orders of magnitude. The photosensitivity of the photo-TFT was improved by adjusting geometrical factors which included the active layer thickness and the channel length as well as the IZO material composition. In particular, the thickness and the composition of the IZO semiconductor strongly influence the degree pf photosensitivity owing to the screening effect of photo-induced V_o^{++}, thereby leading to the generation of back-channel conduction by excess electrons. The IZO material composition affects the interfacial quality as well. Thus, in order to achieve high photocurrent and good TFT characteristics, the bi-layer oxide structure was employed as the active semiconductor channel. This structure as a result achieved the highest photoconductivity of 3×10^4 with a low subthreshold slope of 0.96 V/decade as an optimized bi-layer IZO photo-TFT. We believe that this result is evidence of considerable progress toward a feasible solution-processed photo-sensor.

References

[1] K. Nomura, H. Ohta, A. Takagi, T. Kamiya, M. Hirano, and H. Hosono, Nature 432, 488 (2004).

[2] N. L. Dehuff, E. S. Kettenring, D. Hong, H. Q. Chiang, J. F. Wager, R. L. Hoffman, C. H. Park, and D. A. Keszler, J. Appl. Phys. 97, 64505 (2005).

[3] H. H. Hsieh and C. C. Wu, Appl. Phys. Lett. 91, 013502 (2007).

[4] K. Nomura, H. Ohta, K. Ueda, T. Kamiya, M. Hirano, and H. Hosono, Science 300, 1269 (2003).

[5] E. Fortunato, P. Barquinha, G. Goncalves, L. Pereira, and R. Martins, Solid-State Electron. 52, 443 (2008).

[6] H. Q. Chiang, J. F. Wager, R. L. Hoffman, J. Jeong, and D. A. Keszler, Appl. Phys. Lett. 86, 013503 (2005).

[7] S. Jeon, S. E. Ahn, I. Song, C. J. Kim, U. I. Chung, E. Lee, I. Yoo, A. Nathan, S. Lee, J. Robertson, and K. Kim, Nature Mater. 11, 301 (2012).

[8] S. Jeon, I. Song, S. Lee, B. Ryu, S. E. Ahn, E. Lee, Y. Kim, A. Nathan, J. Robertson, and U. I. Chung, Adv. Mater. 26, 7102 (2014).

[9] P. Barquinha, A. Pimentel, A. Marques, L. Pereira, R. Martins, and E. Fortunato, J. Non-Cryst. Solids 352, 1756 (2006).

[10] E. Fortunato, P. Barquinha, and R. Martins, Adv. Mater. 24, 2945 (2012).

[11] S. -H. K. Park, C. -S. Hwang, M. Ryu, S. Yang, C. Byun, J. Shin, J. -I. Lee, K. Lee, M. S. Oh, and S. Im, Adv. Mater. 21, 678 (2009).

[12] S. J. Kim, S. Yoon, and H. J. Kim, Jpn. J. Appl. Phys. 53, 02BA02 (2014).

[13] S. E. Ahn, I. Song, S. Jeon, Y. W. Jeon, Y. Kim, C. Kim, B. Ryu, J. H. Lee, A. Nathan, S. Lee, G. T. Kim, and U. I. Chung, Adv. Mater. 24, 2631 (2012).

[14] S. Lee, S. Jeon, R. Chaji, and A. Nathan, Proc. IEEE 103, 644 (2015).

[15] Y. H. Hwang, J.-S. Seo, J. M. Yun, H. Park, S. Yang, S.-H. K. Park, and B.-S. Bae, NPG Asia Mater. 5, e45 (2013).

[16] T. Szorenyi, L. D. Laude, I. Bertoti, Z. Geretovszky, and Z. Kantor, Appl. Surface Sci. 96-98, 363 (1996).

[17] G. H. Kim, H. S. Kim, H. S. Shin, B. D. Ahn, K. H. Kim, and H. J. Kim, Thin Solid Films 517, 4007 (2009).

[18] H. S. Choi and S. Jeon, Appl. Phys. Lett. 104, 023505 (2014).

[19] H. S. Choi and S. Jeon, Appl. Phys. Lett. 106, 013503 (2015).

[20] S. W. Shin, K. H. Lee, J. S. Park, and S. J. Kang, ACS Appl. Mater. Interfaces. 7, 19666 (2015).

[21] H. X. Jiang and J. Y. Lin, Phys. Rev. Lett. 64, 2547 (1990).

요 약 (국문 초록)

비정질 실리콘과 저온 폴리 실리콘으로 만든 TFT는 평판 디스플레이 산업에서 널리 사용되고 있지만 많은 단점들을 가지고 있다. 이를 극복할 수 있는 대안으로 산화물 반도체가 대두되어 TFT 활성층으로 사용하기 위해 수년간 꾸준히 연구되어 왔다. 최근 전자기기들은 사용자와 상호작용을 하는 인터렉티브 기술이 폭넓게 이용되고 있다. 가장 대표적인 사례는 TFT 와 sensor 가 결합한 인터렉티브 디스플레이 기술이다. 이러한 관점에서 산화물 반도체는 인터렉티브 디스플레이에서 스위치와 광 센서 역할을 동시에 할 수 있다. 지금까지 대부분의 산화물 포토트랜지스터에 대한 연구는 진공공정으로 만든 산화물 반도체에 집중되어 왔다. 이보다 용액공정으로 산화물 반도체를 제조하면, 매우 단순하고 저비용이며 조성변화가 자유롭다는 여러 가지 장점들을 가지고 있다.

이 논문에서 우리는 용액 공정으로 만든 InZnO 로 산화물 포토트랜지스터를 제작하고 그 특성을 살펴보았다. 빛 에너지를 인가하였을 때, 음의 게이트 전압영역에서 포토전류는 문턱전압의 변화 없이 크게 증가하였다. 빛에 대한 반응성은 기하학적인 요소와 IZO 물질의 조성에 따라 변화되었다. 트랜지스터의 채널 사이즈와 IZO 의 두께에 따른 영향성, 그리고

IZO 조성에 따른 광 반응성 차이를 확인하였는데 이러한 현상은 빛에 의해 이온화된 산소결함의 스크린 효과와 연관된 현상이다. 특히 최적화 된 이중 적층 구조의 IZO TFT 는 광 반응도와 문턱 전압 이하에서의 기울기에서 각각 $3x10^4$, 0.96 V/dec 의 결과를 나타내었다. 또한 산화물 포토 TFT 의 고유 특성인 지속적인 광 반응 현상이 양의 게이트 전압 하에서 제거된다는 것을 확인하였다. 이와 같은 모든 결과들은 용액 공정으로 만든 IZO photo-TFT 가 성공적으로 인터렉티브 디스플레이 제품의 소자로써 역할을 수행할 수 있다는 것을 보여주고 있다.

주요어 : 박막 트랜지스터, 산화물 반도체, 광전 감도,
광 센서, 용액 공정, 산소 결함

학 번 : 2014-24886